NMR Studies on the Conformation of the CD4 36−59 Peptide Bound to HIV-1 gp120†

Dawit Gizachew,‡ Daphne B. Moffett,‡,§ Scott C. Busse,‡ William M. Westler,|| Edward A. Dratz,‡ and Martin Teintze*,‡

Department of Chemistry and Biochemistry, Montana State University, Bozeman, Montana 59717, and NMR Facility at Madison, Biochemistry Department, University of Wisconsin, Madison, Wisconsin 53706

Received March 20, 1998; Revised Manuscript Received June 1, 1998

ABSTRACT: A peptide containing residues 36−59 of the human CD4 receptor includes most of the residues thought to be involved in binding the HIV surface glycoprotein, gp120. This peptide was synthesized and inhibited the binding of gp120 to soluble CD4. NMR relaxation experiments indicated that the peptide was in fast exchange between the free and gp120-bound states. Transferred NOESY NMR showed a number of long-range NOEs, from the gp120-bound state, between residues 38, 40, 45, 48, and 49 of the peptide. NMR evidence also suggested that the Phe43 in the peptide, which corresponds to a critical residue in CD4 for the binding of gp120, makes intimate contact with gp120. The Tr-NOESY cross-peak intensities provided proton−proton distance constraints on the conformation of the gp120-bound peptide. The distance constraints were used in simulated annealing, and a set of 20 very similar structures was obtained for the central region of the gp120-bound peptide. Residues 42−49 of the peptide formed a loop with the side chain of Phe43 pointing away from the rest of the peptide. This Phe43 ring points away from the protein surface in two structures of the amino-terminal domain of CD4 found by X-ray crystallography. Differences in the conformation of CD4 in the two crystal forms suggest that the 36−59 region might be flexible. The NMR data on the 36−59 CD4 peptide predicts a gp120-bound conformation different from either of the CD4 crystal forms in the absence of gp120.

HIV,[1] the human immunodeficiency virus, primarily infects T-lymphocytes bearing the CD4 receptor. HIV infection depletes the body of these $CD4^+$ cells, which are crucial to the proper functioning of the immune system, thereby causing vulnerability to a host of opportunistic pathogens as well as decreasing the ability of the immune system to prevent the spread of the virus. The virus gains entry into CD4-bearing cells as a result of the binding of the viral surface glycoprotein gp120 to both the CD4 receptor (*1*, *2*) and one of several chemokine receptors (*3*−*6*).

Human CD4 is a 435-residue plasma membrane glycoprotein with two N-linked oligosaccharides (*7*); the first 374 residues contain the four extracellular domains, and the C-terminal region contains membrane-spanning and cytoplasmic domains. Recombinant soluble CD4 (sCD4), containing only the extracellular domains, has a high affinity for gp120 ($K_d = 10^{-9}$ M) and can block the infection of $CD4^+$ cells by laboratory strains of HIV in vitro (*8*, *9*). Constructs containing only the first two amino-terminal domains (residues 1−183) have been expressed in bacteria and studied by X-ray crystallography. They were found to have two immunoglobulin-like folds made up of β-sheets (*10*−*12*). The similarities between CD4 and immunoglobulin folds have led to the regions within the domains of CD4 being identified as CDRs (complementarity determining regions) by homology to the corresponding regions in immunoglobulin structures.

Two different crystal forms of the CD4 domain 1+2 fragment have been studied by X-ray crystallography, and their structures have been solved to 2.3 and 2.9 Å resolution (*12*). Differences in the conformations of the surface loops in these two structures suggest that these loops may be somewhat flexible, and thus conformational changes might well occur upon binding to gp120. Evidence for a substantial change in conformation of CD4 upon binding to gp120 comes from the identification of a human recombinant antibody that does not bind CD4-positive cells or HIV-1 envelope proteins, but recognizes and immunoprecipitates cell surface-expressed CD4 after exposure of the cells to gp120 or HIV virions (*13*), and from monoclonal antibodies that have a distinct preference for CD4 complexed to gp120 over free CD4 (*14*). The epitopes of the latter antibodies have been mapped to the CDR2-like region of the N-terminal domain 1 of CD4 (*14*).

† This work was supported by National Science Foundation (NSF) Grant OSR-9350546 to M.T. and E.A.D. NMR studies carried out at the National Magnetic Resonance Facility at Madison were subsidized by NIH Grant RR02301 and used equipment funded by the University of Wisconsin, NSF Grants BIR-9214394 and DMB-8415048, NIH Grants RR02781 and RR08438, and the U.S. Department of Agriculture.

* To whom correspondence should be addressed.

‡ Montana State University.

§ Present address: Centers for Disease Control and Prevention, Atlanta, GA.

|| University of Wisconsin.

[1] Abbreviations: CD4, a protein found on the membrane of helper T-cells, macrophages, and monocytes; HIV, human immunodeficiency virus; gp120, the 120 kDa envelope glycoprotein of HIV-1; NOE, nuclear Overhauser enhancement; NOESY, two-dimensional nuclear Overhauser enhancement spectroscopy; TOCSY, total correlation spectroscopy.

S0006-2960(98)00652-7 CCC: $15.00
Published on Web 07/09/1998

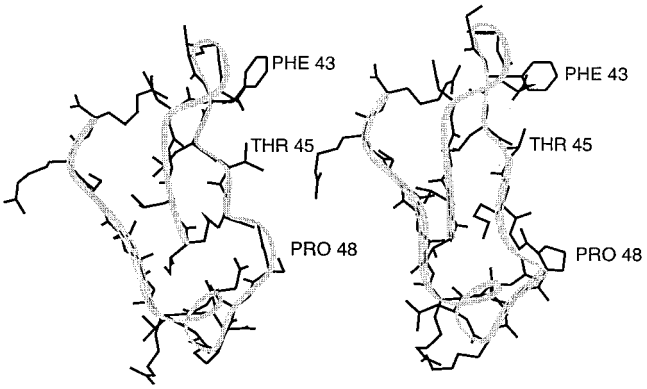

FIGURE 1: Conformation of residues 36−59 in the CDR2 region of CD4 as found in the X-ray structures of two different crystal forms (*12*). Coordinates were obtained from the Brookhaven Protein Data Bank and displayed using Insight97 (MSI, San Diego). The structures are somewhat different, especially in the region of Pro48, suggesting that the structure may be influenced by crystal packing forces and that the conformation of this region may be somewhat flexible.

Extensive studies using site-specific and random mutagenesis of human CD4 have identified residues primarily in the CDR2-like region of domain 1 as important for gp120 binding. Analysis of mutations that affect binding and the X-ray structure of the domain 1+2 fragment of CD4 has suggested that Lys29, Lys35, Phe43, Leu44, Lys46, Gly47, and Arg59 might be involved in direct interaction with gp120 (*12*, *15*). A segment of the two crystal structures in this region is shown in Figure 1. The Phe43 side chain is pointing out toward the solvent in both crystal forms, as if it were poised to fit a hydrophobic binding pocket. However, this Phe side chain interacts with neighboring CD4 molecules in the crystals (*12*), and the orientations of the side chains on the contact surfaces between the proteins in the crystals may not reflect their behavior in the biologically relevant CD4−gp120 complex. Phe43 is particularly important for gp120 binding: Substitution of Phe43 by Leu, Trp, or Tyr results in 2.5-, 16-, and 32-fold decreases in binding affinity for gp120; substitution by Ala, Ile, and other amino acids results in a >500-fold decrease in binding affinity (*15*). Rat CD4 has <50% identity with the human sequence and does not bind gp120. However, substitution of residues 34−61 from the human CD4 sequence into rat CD4 protein imparts significant gp120 binding affinity to the chimeric protein (*16*), confirming the importance of this CDR2 region in the interaction between human CD4 and gp120.

A detailed understanding of the gp120−CD4 receptor interaction at the molecular level should be helpful toward elucidating the mechanism of HIV entry into the cell and could facilitate the design of drugs that block infection. Understanding the three-dimensional structure at the sites of the gp120 and CD4 interaction is an important step toward these goals. Surface loops of proteins involved in binding may be quite flexible (*17*, *18*), and structures of the isolated CD4 domains in crystals may not reflect the shape of the binding interface when CD4 is bound to gp120. To obtain information about the gp120-bound conformation of CD4, we have identified a CD4 peptide that blocks the interaction with gp120 and have used transferred NOESY NMR spectroscopy to study the conformation of the peptide when it is bound to gp120.

MATERIALS AND METHODS

Peptide Synthesis and Purification. Four peptides were made using a Milligen/Perseptive Biosystems 9050 continuous flow peptide synthesizer and Fmoc amino acids. Peptides **2** and **3** were N-acetylated with acetic anhydride prior to deprotection of the side chains and cleavage from the resin. The peptides were purified by reverse-phase HPLC with dual absorbance monitoring and analyzed by both electrospray and laser desorption time-of-flight mass spectroscopy.

Proteins. The $gp120_{SF2}$ used in the NMR experiments was produced in Chinese hamster ovary (CHO) cells (*19*) and generously provided by the Chiron Corp. (Emeryville, CA). $gp120_{IIIB}$ produced in baculovirus-infected insect cells was purchased from Intracel (Cambridge, MA). Recombinant soluble CD4 (sCD4) containing the two amino-terminal domains (residues 1−183), originally produced in *Escherichia coli* by Upjohn (Kalamazoo, MI), was a gift from Dr. Seth Pincus.

ELISA Assays. The affinity of peptides for gp120 and their ability to block the gp120−CD4 interaction were measured using a gp120 capture ELISA assay. The kit used for the assay (Intracel; Cambridge, MA) contains an ELISA plate coated with sCD4, a solution of $gp120_{IIIB}$, and a monoclonal antibody to gp120 that does not interfere with CD4 binding, conjugated to horseradish peroxidase. Tetramethylbenzidine was used as the peroxidase substrate, and the plates were read at 450 nm using a BIOTEK EL-311S microplate reader. This ELISA kit was able to detect gp120 in samples at levels ranging from 1 to 500 ng. Peptides at concentrations between 1 μM and 3 mM were mixed with 32 ng of gp120 in 0.1 mL and added to the sCD4-coated wells on the ELISA plate along with controls containing only gp120 or only peptide. ELISA assays were also carried out using gp120-coated plates; in this case, sCD4 binding was detected using rabbit antibodies to CD4 and alkaline phosphatase-conjugated secondary antibodies (*20*−*22*). For these assays the plates were coated with either $gp120_{IIIB}$ made in insect cells or $gp120_{SF2}$ made in CHO cells. The latter protein did not bind sCD4 when it was attached directly to the wells; this problem was overcome by coating the wells with the lectin concanavalin A and binding the $gp120_{SF2}$ to the conA. This method resulted in sCD4 binding equivalent to that observed with $gp120_{IIIB}$ plates.

Circular Dichroism. Peptide **3** (1.5 mM) in 25 mM sodium phosphate, pH 6.0, was placed in a cuvette with 0.1 mm path length, and CD spectra were measured from 280 to 190 nm on a JASCO J-720 instrument at room temperature. CD values from 200 to 240 nm were used with the K2d algorithm (*23*, *24*) to fit the spectra to a fraction of α-helix, β-sheet, and random coil.

NMR Sample Preparation. For the free peptide NMR experiments, 2 mM peptide **3** was dissolved in PBS (150 mM NaCl, 25 mM sodium phosphate) and the pH adjusted to 6.0 with NaOH. The $gp120_{SF2}$ was centrifuged repeatedly at 4 °C in a Centricon 30 concentrator (Amicon) and rediluted with PBS, pH 6.0, to remove the citrate buffer in which the protein was provided and to concentrate the protein. 1D NMR spectra were run to check for the absence of sharp proton signals from small molecules; the centrifugal filtration and washing process was repeated until no sharp peaks were observed. The gp120 concentration was determined by

absorbance at 280 nm and ELISA assays. Solid peptide **3** was dissolved in the protein solution, and the pH was adjusted to 6.0; 5% D_2O and 3-(trimethylsilyl)propionic-*2,2,3,3-d*$_4$ acid (sodium salt) were included in all samples to provide lock and reference signals, and 0.02% NaN_3 was added to inhibit microbial growth. Final concentrations in the bound peptide samples were 2 mM peptide and 66 μM $gp120_{SF2}$.

NMR Measurements. All spectra were recorded at 5 °C. 2D spectra were measured in the phase-sensitive mode in the indirect dimension using the TPPI method (*25*). Initial spectra were performed on a Bruker AM500 spectrometer at MSU. Transferred NOESY (Tr-NOESY) spectra (*26*−*28*) of the bound peptide sample were taken at six different mixing times from 75 to 500 ms with jump-and-return detection to avoid excitation of water. Some of the Tr-NOESY spectra were acquired with a 2 ms spin−echo filter in front of the t_1 evolution time (*29*) to refocus the magnetization of the peptide ligand while randomizing the magnetization of the protein to remove broad protein background from the spectra. $T_{1\rho}$ relaxation times (T_1 relaxation times in the rotating frame) were measured on the free and the bound peptide with the spin−lock frequency centered on peaks that shifted upon addition of protein to the peptide. The log of the peak intensity was plotted as a function of spin−lock duration. The spin−lock duration was varied over a range of 2−400 ms at several spin−lock power levels from 15 to 75 dB attenuation, which corresponded to spin−lock frequencies of 8155−8.2 Hz, to assess off rates (*30*).

The structural information in Tr-NOESY is measured on the sharp spectra of the free peptide, and there was considerable spectral overlap at 500 MHz. Therefore, higher resolution spectra were acquired on a Bruker DMX750 at the NMR Facility in Madison, WI (NMRFAM), using a 5 mm proton-selective, triple resonance, three-axis gradient probe. These spectra were used to make final resonance assignments and to measure more resolved NOESY cross-peak intensities. TOCSY spectra on the free and bound peptide samples were recorded using the MLEV-17 pulse sequence (*31*). NOESY spectra were collected using a 200 ms mixing time and triple-axis gradients with watergate for water suppression. A total of 8192 complex data points in t_2 were collected for 512 t_1 increments. The spectral assignments were confirmed using natural abundance $^{13}C-^{1}H$ heteronuclear single-quantum coherence spectroscopy (HSQC) on a Bruker DRX500 at MSU. Spectra were processed using FELIX95 software (MSI, San Diego). Some of the 750 MHz NOESY spectra were recorded with a spin−echo filter in front of the t_1 evolution time (as described above for the 500 MHz spectra) as well as four equally spaced spin−echos, each preceded by a $\pi/2$ flip-back pulse and followed by a $\pi/2$ restoration pulse, applied during the mixing time. These spin−echo filters randomize the protein magnetization, refocus the peptide magnetization, and restore the peptide magnetization to the longitudinal axis for additional mixing and cross-relaxation. Perturbing the relative magnetization during the mixing time in this way is a form of magnetization exchange network editing (*32*), which reduces but does not eliminate protein proton mediation of ligand Tr-NOESY (E. A. Dratz, unpublished).

Structure Calculations. Structures of the gp120-bound peptide based on distance constraints from the Tr-NOESY experiments were calculated by simulated annealing (*33*). The distance constraints were derived as described in the Results section below. Twenty sets of randomized coordinates from the extended conformation were used as starting structures. For each starting structure, two steps of molecular mechanics calculations were followed by a molecular dynamics calculation for 30 ps with a 1 fs time step at a temperature of 700 K and very low force constants. The temperature was then lowered to 650, 475, 385, 340, and 300 K, and molecular dynamics calculations were continued for 2 ps each, while increasing the force constants to full scale. Molecular mechanics calculations were then run, until convergence was reached at 0.01 kcal/Å, to generate 20 structures.

RESULTS

Initial Characterization of CD4 Peptides. Four different peptides corresponding to overlapping sequences in the CDR2 region of CD4 were synthesized, each of which contained a different subset of the residues predicted to be most important for binding to gp120. These peptides were assayed for their ability to block the gp120−CD4 interaction by ELISA.

Peptide **1**, GNQGSFLTKGPSKLNamide (CD4 residues 38−52), was soluble in water up to 5mM. Peptide **1** did not show reproducible effects on the binding of gp120 to the CD4 plate in the ELISA assay at concentrations tested (up to 2.5 mM) and was therefore not used in NMR experiments. Weak binding of peptides to gp120 (K_d of >1 mM) would not have been detected by the competition ELISA due to the high affinity of CD4 for gp120 (K_d = 1 nM).

Peptide **2**, AcQIKILGNQGSFLTKGPamide (CD4 residues 33−48), was poorly soluble in aqueous solutions under a variety of conditions and was not studied further.

Peptide **3**, AcILGNQGSFLTKGSPSKLNDRADSRRamide (CD4 residues 36−59), was soluble to 6 mM. Peptide 3 showed inhibition of CD4−gp120 binding in ELISA assays, with an IC_{50} of about 2 mM. Given the uncertainties in the effective concentrations of the CD4 (or gp120) that was immobilized on the ELISA plate used for the peptide competition assay, the K_d for peptide **3** bound to gp120 was estimated to be between 100 and 500 μM. This range of binding affinity made the peptide likely to be suitable for Tr-NOESY NMR experiments, which require fast exchange between the free and bound states. Peptide **3** was therefore chosen for further investigation in NMR experiments described below.

Peptide **4** (CD4 residues 16−49) has previously been reported to compete with monoclonal antibodies that block the CD4 binding site on gp120 and inhibit the formation of syncytia in cells expressing CD4 and gp120/gp41 at concentrations down to 50 μM (*34*), and we investigated this sequence also. Its length (34 residues) and the presence of five lysine residues made it a more difficult target for study of its gp120-bound structure by Tr-NOESY NMR than peptide **3**. ELISA assays with this peptide resulted in very high background, even in control wells that were not coated with gp120. Peptide **4** was therefore binding nonspecifically

Table 1: Resonance Assignments for the Gp120-Bound Peptide **3**

residue	NH	αH	βH	γH	other side chain
N-acetyl		2.041			
Ile36	8.368	4.112	1.844	1.205, 1.478	γCH_3 0.910, δ 0.875
Leu37	8.558	4.400	1.689	1.585	δ 0.907
Gly38	8.538	3.964			
Asn39	8.526	4.730	2.828, 2.840		NH_2 7.038, 7.741
Gln40	8.703	4.322	2.040, 2.198	2.404	NH_2 7.013, 7.655
Gly41	8.586	3.950			
Ser42	8.253	4.420	3.797		
Phe43	8.380	4.642	3.055, 3.198		δ 7.264, ϵ 7.365
Leu44	8.286	4.388	1.649	1.568	δ 0.882, 0.896
Thr45	8.219	4.329	4.229	1.246	
Lys46	8.506	4.394	1.792, 1.900	1.338, 1.447	δ 1.668, ϵ 3.005
Gly47	8.458	4.054, 4.169			
Pro48		4.478	1.963, 2.314	2.042	δ 3.646
Ser49	8.669	4.438	3.885		
Lys50	8.653	4.354	1.777, 1.900	1.476	δ 1.725, ϵ 3.008
Leu51	8.410	4.301	1.648	1.606	δ 0.891
Asn52	8.565	4.701	2.773, 2.882		NH_2 7.049, 7.772
Asp53	8.365	4.581	2.696		
Arg54	8.403	4.323	1.822, 1.938	1.656	δ 3.221, NH 7.461
Ala55	8.507	4.254	1.417		
Asp56	8.453	4.597	2.743		
Ser57	8.387	4.394	3.910, 3.979		
Arg58	8.412	4.325	1.813, 1.915		δ 3.226, NH 7.403
Arg59	8.383	4.313	1.814, 1.904	1.664	δ 3.233, NH 7.337
C-amide	7.290, 7.677				

both to the plate and to the sCD4 or the anti-CD4 antibodies. These data suggested the possibility that biological effects reported for this peptide may have been the result of nonspecific binding to HIV-infected cells. These properties greatly hampered the characterization of peptide **4** binding and made it a poor choice for further experimentation.

*CD Spectra of Peptide **3**.* The CD spectrum of peptide **3** had the characteristics of model peptides considered to be "random coils" without secondary structures, and the K2d program calculated the best fit as 98% random coil and 1% each of α-helix and β-sheet.

Assignment of Peptide Resonances. TOCSY and NOESY cross-peak connectivities in the spectra of the free and gp120-bound peptide **3** were used to identify the spin systems of residues. Sequential assignments were made using the NOEs between the α-carbon protons of residue *i* and the amide protons of residue $i+1$ [$d_{\alpha N}(i, i+1)$]. A crucial factor for NMR structure determination is correct signal assignment, and many signals overlapped at 500 MHz. However, at 750 MHz, the NOESY cross-peaks were sufficiently well resolved and additional cross-peaks were detected, allowing assignment of all backbone resonances, including the *N*-acetyl and C-terminal amide groups, and all side chain α- and β-carbon protons (Table 1). The presence of three Leu, three Arg, and two Lys residues made specific assignment of some γ, δ, and ε carbon protons in those side chains difficult. More than 180 NOESY cross-peaks were assigned in the bound peptide NOESY spectrum. Intraresidue and sequential residue NOEs were observed for all 24 residues in the peptide. Regions near the N-terminal and C-terminal ends of the peptide did not show long-range NOEs, but some long-range NOEs were observed between protons in the region from residues 38 to 49 of the bound peptide (Figure 2; see below). The cross-peaks due to Gln40 Hβ1, Pro48 Hγ, and the acetyl group protons at the N-terminal of the peptide could not be resolved at 2.04 ppm in the f_1 (D_2) dimension (Figure 2B) but were clearly distinct in the f_2 (D_1) dimension on the other side of the diagonal (Figure 2C). Assignments were confirmed using a natural abundance $^{13}C-^{1}H$ HSQC spectrum of peptide **3** (data not shown).

Measurement of Cross-Relaxation Rates in the Bound Peptide. The buildup of normalized NOE intensity as a function of mixing time was examined for a number of proton pairs in the bound peptide. Intensities were measured for the Gln40 side chain amide, Phe43 β-CH_2, Gly47 α-CH_2, and C-terminal amide protons, because these had among the fastest cross-relaxations, and they were corrected for the contributions of the free peptide. The normalized NOE buildup was linear at mixing times up to 150 ms. Cross-relaxation rates for these protons were estimated to be ∼20/s at the 75 ms mixing time.

Measurement of the gp120−Peptide Dissociation Rate. Some of the peptide **3** protons showed small chemical shifts when gp120 was added, consistent with fast exchange of the bound peptide on the chemical shift time scale. In fast exchange, the resonance position observed is a weighted average of the chemical shifts in the bound and unbound state. Spin−lock irradiation was centered on a peak that showed a shift when gp120 was added. As the spin lock power is decreased, the spin lock loses its effectiveness if the spin−lock frequency approaches the k_{off} frequency. As the spin−lock frequency changes from being faster than k_{off} of the peptide from the protein to slower than k_{off}, the chemical shift of the proton is modulated between the bound and free frequencies, so the exchange tends to defeat the spin−lock and causes faster relaxation in the rotating frame. The off rate for the peptide dissociation from gp120 was estimated by measuring the $T_{1\rho}$ at different spin−lock powers and plotting $1/T_{1\rho}$ vs the log of the spin−lock frequency (*30*). The frequency at the midpoint between the fast and slow relaxation rates was then used to estimate k_{off} (*30*), which was about 200−500/s in the bound peptide. No change in $T_{1\rho}$ relaxation rates was observed for the protons in the free peptide, as a function of spin−lock power. Since the k_{off}

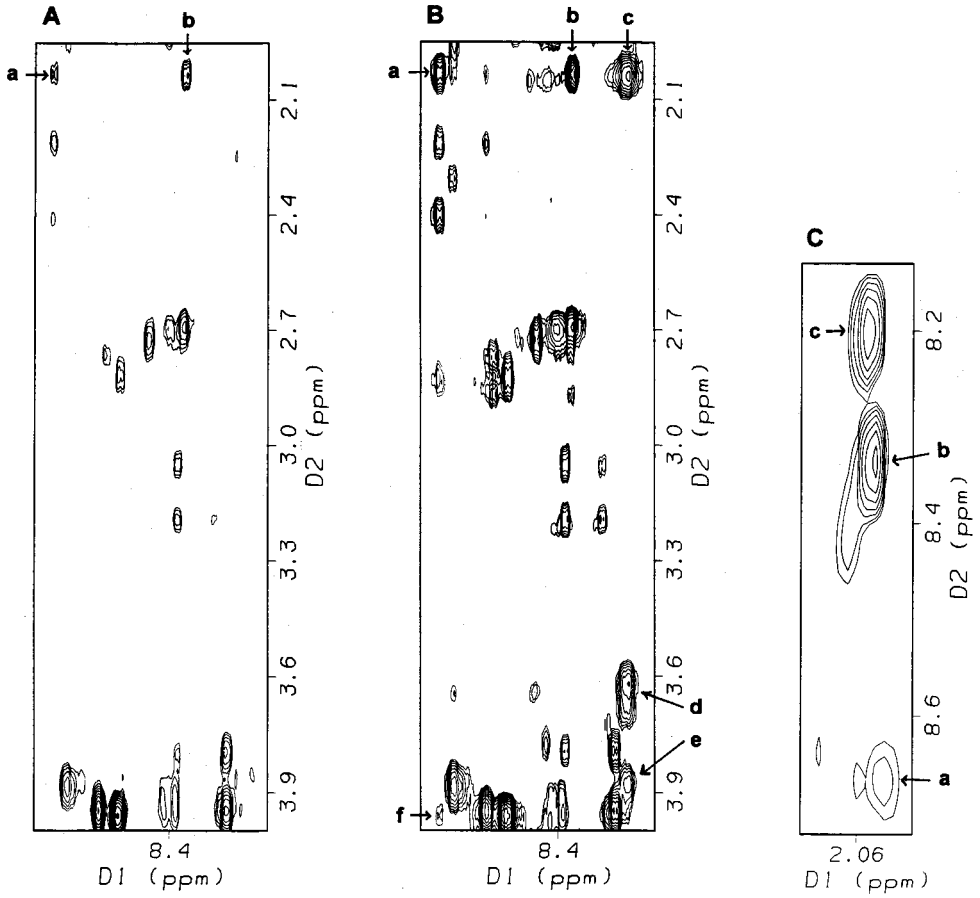

FIGURE 2: Regions of the peptide **3** NOESY spectra at 200 ms mixing time, showing long-range NOESY cross-peaks that appear upon addition of gp120. Panels: A, free peptide **3**; B and C, gp120-bound peptide **3**. Selected assignments are marked as follows: a, Gln40 HN−Hβ1; b, Ile36 HN−*N*-acetyl group; c, Thr45 HN−Pro48 Hγ; d, Thr45 HN−Pro48 Hδ; e, Thr45 HN−Ser49 Hβ; f, Gln40 HN−Gly38 Hα.

was an order of magnitude faster than the fastest cross-relaxation rates in the bound peptide, the NOE cross-peak intensities observed should be essentially free of effects due to slow exchange (*35*).

*Conformation of the gp120-Bound Peptide **3***. Since the peptide is in fast exchange on the cross-relaxation time scale of the bound peptide, the observed Tr-NOESY intensities are sums of the bound and free peptide NOEs (*36*). The NOE cross-peak intensities in the bound and free spectra were normalized by their diagonal intensities (*37*), and the bound peptide NOESYs were obtained by subtracting any contribution of the free peptide NOESYs. Using the ratio of peptide to gp120 in the sample and a dissociation constant estimated at 100−500 μM, the fraction of the peptide bound to gp120 (f_b) was estimated at 2.5−3%. A full-relaxation matrix analysis was performed using the program MARDIGRAS 2.3 (*38*, *39*) to account for spin diffusion among the bound peptide protons. Using a correlation time of 40 ns for the gp120-bound peptide in MARDIGRAS, with an effective mixing time of $f_b t_{mix}$, gave the most reasonable interproton distances for proton pairs attached to the same atom, and this value also agreed well with the correlation time estimated from the size of gp120. (Lists of cross-peak intensities and the distance constraints derived from them are given in Supporting Information).

The presence of many strong $d_{\alpha N}(i, i+1)$ cross-peaks, but few $d_{NN}(i, i+1)$ and no $d_{NN}(i, i+3)$ cross-peaks in both free and bound NOESY spectra, indicated that the bound peptide had a predominantly extended chain and provided no evidence for α-helical regions. In the gp120-bound state, long-range NOEs were observed between Gly38 and Gln40, as well as between Thr45 and both Pro48 and Ser49 (Figure 3). No long-range NOEs were observed in the free peptide. The cross-peaks between the Thr45 HN and the Pro48 Hγ and Hδ protons (Figure 2) were very strong, indicating very close proximity between these residues in the bound structure. Cross-peaks between the Gly47 Hα protons and the Pro48 Hδ protons, but not the Pro48 Hα protons, indicated that Pro48 was in the trans configuration (*40*). Residues 45−48 are constrained by these long-range NOEs to form a loop in the bound peptide, but there is no evidence for a typical β-turn in this region. Residues 38−41 have NOE connectivities that suggest the presence of a type II β-turn or a half-turn: a medium $d_{NN}(i, i+1)$ between Asn39 and Gln40, a medium−strong $d_{\alpha N}(i, i+1)$ between Gly38 and Asn39, and a weak $d_{\alpha N}(i, i+2)$ between Gly38 and Gln40 (*41*, *42*).

Simulated annealing experiments, using the distance constraints obtained from MARDIGRAS, were performed on the full-length peptide **3**, starting with 20 sets of randomized coordinates generated from an extended chain conformation, as described in Materials and Methods. The carboxyl-terminal region of the peptide (residues 50−59) had no long-range NOEs and was not well constrained by the Tr-NOESY data. For most of the 20 model structures, residues 50−59 were in an extended chain conformation, but since small kinks in a chain of this length result in large

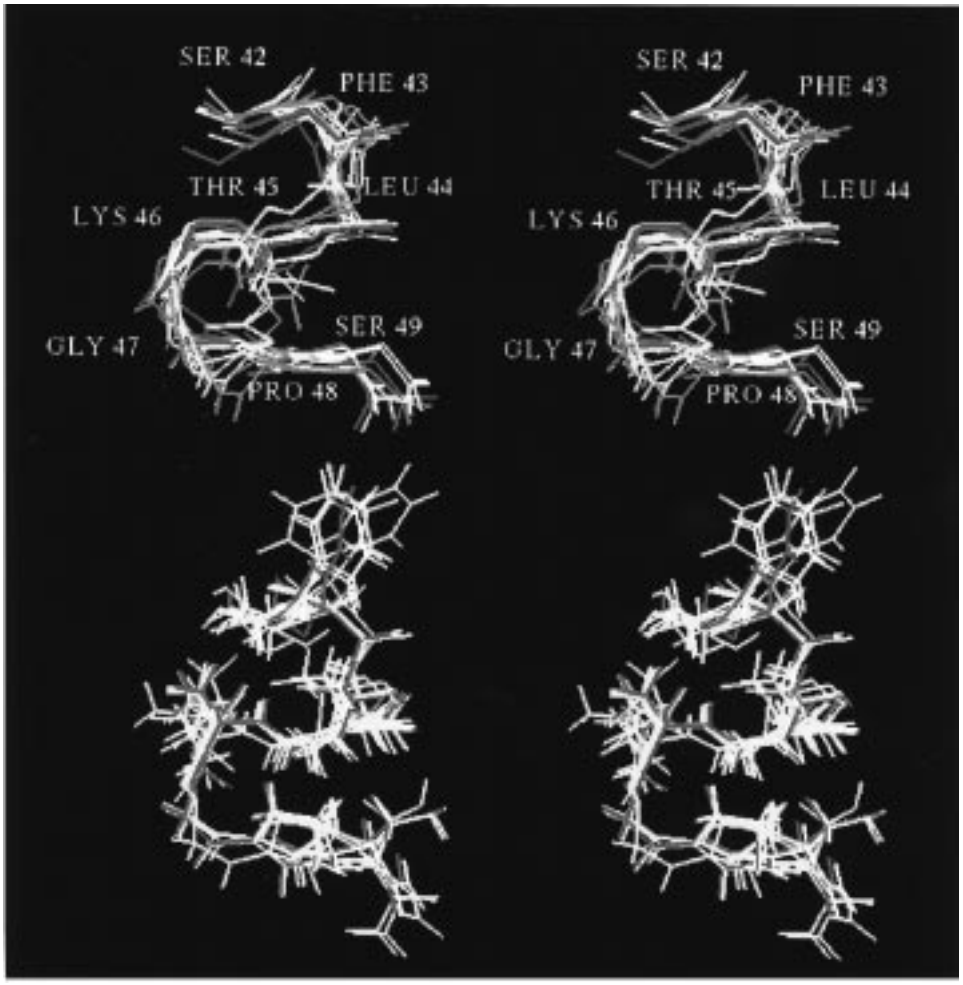

FIGURE 3: Stereoviews of the region encompassing residues 42−49 from 13 of the 20 structures of the gp120-bound peptide **3** obtained by simulated annealing. (Top) Backbone atoms only. (Bottom) All atoms for 6 of the structures displayed to show the side chain orientations.

differences in the position of the carboxyl-terminal residues, these structures did not superimpose well. Therefore, simulated annealing was also carried out on only the amino-terminal 14 residues, using 107 NOE distance constraints (4 long-range and 42 medium range) and starting with 20 sets of randomized coordinates generated from an extended chain conformation of residues 36−49. Very good convergence was observed in the region encompassing residues 42−49 of the peptide, for which there were 81 NOE distance constraints (3 long range and 33 medium range).

The resulting structures were superimposed using the program Insight97 (MSI, San Diego). Most of the model structures generated from residues 36−49 showed very similar backbone structures in the region from residues 42 to 49, as shown in Figure 3, with an average rms backbone deviation of 1.04 Å from one of the calculated structures with the lowest energy. These structures were used to back-calculate the predicted NOE intensities using the program CORMA 5.2 (*38*, *39*). The NOEs calculated from the interproton distances were in good agreement with the observed NOEs in the bound peptide (Figure 4). The average rms deviation of the structures for all the atoms in residues 42−49 was 2.21 Å; this is much larger than the backbone deviation, as expected, due to the lack of constraints on the orientation of many of the side chains. There were a few NOEs calculated from the structures that were not observed, but these primarily involved side chain conformations.

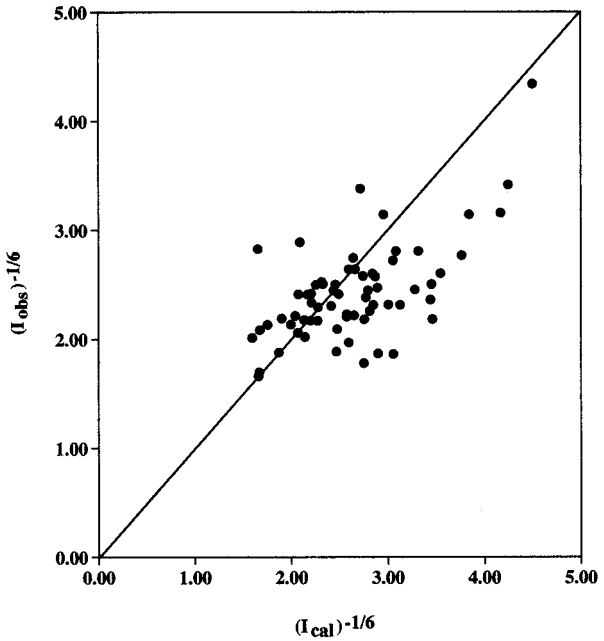

FIGURE 4: Comparison of observed NOESY distance constraints for residues 42−49 of gp120-bound peptide **3** and the NOESY distance constraints calculated from a selected low-energy structure.

Additional molecular dynamics calculations were done, with these proton pairs constrained to be between 4.5 and 30 Å

apart. The resulting structures had some of the side chain orientations more constrained, but the backbone conformations of the residue 42−49 region were not significantly different from those shown in Figure 3.

The Phe43 side chain varied in orientation between the structures shown in Figure 3, because there were no NOEs between the ring protons and those of any other residue in the peptide. However, the main chain constraints dictated that the Phe side chains in all the structures were oriented away from the remainder of the peptide. Evidence from spin−echo experiments, described below, suggested that the Phe side chain may be contacting the gp120 protein, as predicted by the mutagenesis and X-ray crystallography studies discussed previously. The region of the peptide from residues 38 to 41 appeared to clearly make another loop, with interproton distances consistent with a type II β-turn in most of the structures. This could represent a nascent turn in the bound conformation, but it was not as well constrained by the NMR data as the residue 42−49 region. The 20 structures calculated did not superimpose sufficiently well in the region from residues 38 to 41, especially for the side chains, to allow clear visualization of the turn in a figure (data not shown).

Spin−Echo Effects on the NOESY Spectra. Spin−echo-filtered NOESY spectra of peptide **3** bound to gp120 were recorded both at 500 MHz using a 2 ms spin−echo before t_1 and at 750 MHz using a 2 ms spin−echo before t_1 and four equally spaced 2 ms spin−echos during the mixing time (see Materials and Methods). The 2 ms spin−echo time allows refocusing of the peptide proton spins, which have a relatively long T_2 (∼200 ms), but not those of the protein, which have a short T_2 and rapidly become dephased with near zero net magnetization. The spin−echo before the t_1 evolution time reduces the broad protein background in the Tr-NOESY (*29*). The flip-back, spin−echo, flip modules in the mixing time randomize the protein proton magnetizations and reduce the protein mediation of ligand Tr-NOESY cross-relaxation. Most of the Tr-NOESY intensities were not significantly affected by the spin−echos, including all the NOEs important for constraining the structure of the bound peptide. However, a few of the intensities decreased by more than a factor of 2 when the spin−echo filter sequence was used, suggesting that there may be substantial cross-relaxation involving the protein for these pairs of ligand protons (data in Supporting Information). In a model system consisting of a biotin-mimetic peptide binding to streptavidin, for which a crystal structure of the complex is available, the peptide proton cross-peaks in the Tr-NOESY spectrum that were affected by the spin−echo filter in this manner were in close contact with the protein (D. Gizachew and E. Dratz, unpublished). The peptide **3** protons most affected by the spin−echos were those on the Phe43 side chain, which would support the hypothesis that this region of the peptide is in contact with gp120. The intensity of the cross-peak due to the Phe ring δ and ϵ protons in the 750 MHz spectra decreased by a factor of 7 when the spin−echo filters were used. This corresponded to an increase in the calculated distance between the δ and ϵ protons from 1.55 to 2.11 Å; the longer distance, obtained using the spin−echo filter, was much closer to the expected distance of 2.47 Å, suggesting that a relay of the magnetization via a closely bound protein proton had been contributing substantially to the cross-peak intensity in the absence of the spin−echos.

Table 2: Changes in Normalized Cross-Peak Volumes upon Addition of sCD4 for Long-Range NOEs and Selected Short-Range NOEs[a]

assignment	% change + sCD4 without spin−echos	% change + sCD4 with spin−echos	fraction of peak due to bound conformation[b]
T45 HN−P48 Hδ	−35	−29	1.0
T45 HN−P48 Hγ	−16	−47	1.0
T45 HN−S49 Hβ	−36	−29	1.0
Q40 HN−G38 Hα[c]	−85	ND	1.0
Q40 HN−Hγ	−51	−49	0.8
Q40 HN−Hα	−8	−16	0.1
G41 HN−Hα	−21	+8	0.2

[a] The intraresidue NOEs shown were selected on the basis of having relatively large volumes that were due primarily either to the bound or to the free peptide. Most of the short-range NOEs had fractional contributions from the bound peptide and percent decreases upon addition of the sCD4 intermediate between the values of the peaks selected for inclusion in this table. [b] $(I_{\text{peptide+gp120}} - I_{\text{free peptide}})/I_{\text{peptide+gp120}}$ in the absence of sCD4. [c] This was a very small peak with a relatively large volume uncertainty; it could not be measured in the spectra with spin−echos, which have weaker intensities for all peaks.

Effect of Competition with sCD4 on NOESY Spectra. To confirm that the bound conformation observed for peptide **3** was induced by binding specifically to the CD4 binding site on gp120, a competition experiment with sCD4 was performed. A sample containing 2 mM peptide **3** and 66 μM $gp120_{SF2}$ was first used to obtain Tr-NOESY spectra at 750 MHz, both with and without spin−echos (see above); then lyophilized sCD4 was added to achieve a final concentration equivalent to that of gp120 (66 μM) and the spectra were repeated. The normalized peak intensities before and after addition of the sCD4 were compared. The long-range NOEs, and those whose intensities were primarily due to the contributions of the gp120-bound peptide, decreased in intensity when sCD4 was present, whereas cross-peaks whose intensity was primarily due to the free peptide NOEs were not significantly affected (see Table 2). The addition of sCD4 decreased the intensities of most of the NOEs due to the bound state of the peptide by about 30−50%. This was in the range of expected values, since the ELISA data had shown about 50% inhibition of sCD4 binding to gp120 at the 2 mM peptide **3** used in the NMR experiments. Most of the Tr-NOESY cross-peaks showed the expected pattern of intensity decreases upon addition of sCD4. Among the long-range NOEs, the intensity of the Thr45 HN−Pro48 Hγ decreased by only 16% in the absence of spin−echos but by 47% when spin−echo filters were used (see Table 2). There was evidence for underlying intensity in this region in the presence of sCD4, most likely due to resonances from mobile regions of the sCD4 protein, which was removed by the spin−echo filter. Addition of sCD4 to the sample also caused increases in intensities for a few peaks and the appearance of some new cross-peaks that could not be assigned. These may have been due to interactions between peptide **3** and sCD4 and to protons on sCD4 with correlation times fast enough to generate sharp peaks.

DISCUSSION

The interaction between HIV gp120 and the CD4 receptor is an important potential target for HIV therapy. This

protein−protein interaction is the first step in the infection of T-cells, macrophages, monocytes, and other cells that carry the CD4 receptor on their surface, and the infection of these cells is responsible for the loss of immune system function that gives rise to the symptoms of AIDS. HIV infection elicits an immune response from the host, but the rapid generation of new variations in the sequence of the envelope glycoprotein gp120 contributes to the ability of the virus to overcome this immune response. Many of the neutralizing antibodies that arise early in HIV infections, and those that are readily generated in animals immunized with gp120, are directed at linear determinants in the highly variable V3 loop of gp120 (*43*, *44*) and neutralize only a limited number of HIV strains (*45*). Mutations arising in this region of the sequence can also readily generate viruses that are no longer neutralized by such antibodies (*46*, *47*). Late in the course of HIV-1 infection of humans, antibodies with broader specificity for different HIV isolates appear (*48*−*50*). Most of these broadly specific antibodies recognize discontinuous epitopes, including the CD4 binding site (*51*−*53*). HIV variants that are no longer able to recognize and bind CD4 would not readily be able to infect new cells and propagate.

Evidence from mutagenesis, peptide competition, and epitope mapping of anti-gp120 and anti-CD4 antibodies indicates that gp120 and CD4 appear to interact over a relatively small fraction of their surfaces (*12*, *14*, *54*−*57*), suggesting that small molecule inhibitors of their interaction might be designed. Attempts to use sCD4 as an HIV neutralizing drug have not been successful in clinical trials. Apparently, high concentrations of sCD4 are needed to neutralize primary HIV isolates (*47*, *58*), and the combination of rapid sCD4 degradation in vivo and its inability to effectively penetrate all tissues that serve as HIV reservoirs may have kept its concentration below the levels needed to neutralize HIV. A small molecule inhibitor may have better pharmacological properties and therefore be more effective than sCD4 was clinically.

Unbound peptide **3** appeared to be essentially a random coil in solution, but we found that it was conformationally constrained in a part of its sequence upon binding to gp120. A random coil peptide in solution binding in a constrained conformation would result in an unfavorable entropy of binding. Thus the enthalpy of binding must be quite favorable indeed to produce a binding constant in the range of 100−500 μM, as was observed for the flexible, linear peptide **3**. Studies on a linear biotin-mimetic peptide binding to streptavidin have shown that the enthalpy of binding is similar to that of biotin, but the unfavorable entropy of peptide binding results in a much lower affinity than that of biotin (*59*). Conformationally constrained biotin-mimetic peptides have a greatly elevated affinity (*60*), compared to similar linear sequences; therefore, conformationally restricted mimics of the bound peptide **3** structure shown in Figure 3 would be expected to have a much higher affinity for gp120 than the linear peptide **3**.

The Phe43 residue in CD4, which is critical for gp120 binding, is located in the fourth position of a β-turn in both crystal forms (*12*). A conformationally locked mimetic of the β-turn from Gln40 to Thr45, which includes Phe43, has been synthesized (*61*). This mimetic was reported to have a K_d for gp120 binding of 5−20 μM and inhibited syncytium formation by 50% at 300 μM. This molecule was designed to mimic the X-ray crystal structure of CD4 domain 1 in the region of this β-turn; two minimum energy conformers are predicted for this mimetic, one of which resembles the structure of the β-turn in CD4 (*61*). The β-turn mimetic is rather small and does not include several of the residues identified as critical for binding by site-specific mutagenesis or the Pro48 and Ser49 residues that appear to be important for the gp120-bound conformation in the NMR studies reported here. Nevertheless, the more favorable entropy of binding dramatically increased the affinity of the constrained mimetic compared to that of the corresponding linear peptide, which showed no measurable inhibition of gp120−CD4 binding (*61*).

Our studies suggest that the gp120-bound conformation of the CDR2 region of CD4 may be somewhat different from the crystal structure, although it is consistent with the proposed role of Phe43 in binding to a hydrophobic pocket on gp120. The structures calculated from our NMR data differ most from the crystal structures of CD4 in the region around Pro48, which is also the location of the largest differences between the two crystal forms of CD4 (*12*). The NMR data supporting a gp120-bound conformation different from those in the crystal structures are also consistent with the immunological evidence for changes in this region of the CD4 structure upon binding to gp120 (*14*). Additional NMR studies are expected to produce more tightly defined bound peptide conformations that may be used as more refined templates for the design of conformationally restricted, higher affinity inhibitors of the gp120−CD4 interaction.

NOTE ADDED IN PROOF

After this paper was accepted for publication, an X-ray crystallographic study was reported of a complex containing a "core" of gp120, domains 1 and 2 of sCD4, and an antibody to gp120 (*62*). In this complex, most of the contacts with gp120 involved the span from residues 40−48 of CD4, and the Phe43 side chain protrudes into a deep cavity in gp120, which is consistent with the gp120-bound CD4 36−59 peptide structure in solution and the NMR spin-echo filtering data presented in our paper. The authors report that the positions of CD4 residues 41, 42, 47, 49, and 60 differ between the X-ray structure of the complex and the previously reported free CD4 structures, but a detailed comparison between our proposed conformation for this region of the complex in solution and the new X-ray structure will not be possible until the X-ray coordinates become available.

ACKNOWLEDGMENT

We thank the late Dr. Kathelyn Steimer and the Chiron Corp. for their generous gift of gp120 for these studies, as well as Dr. Seth Pincus and the Upjohn Co. for sCD4. We also thank Drs. Joan Cory and Seth Pincus for helpful discussions, Craig Johnson for peptide synthesis and purification, and the staff of the NMR Facility at Madison for assistance with NMR experiments.

SUPPORTING INFORMATION AVAILABLE

Peptide **3** NOESY cross-peak assignments and intensities, peptide **3** + gp120 NOESY cross-peak assignments and intensities, NOE distance constraints used for simulated

annealing experiments, and peptide **3** + gp120 spin−echo NOESY cross-peak intensities (15 pages). Ordering information is given on any current masthead page.

REFERENCES

1. Maddon, P. J., Dalgleish, A. G., McDougal, J. S., Clapham, P. R., Weiss, R. A., and Axel, R. (1986) *Cell 47*, 333−348.
2. Sattentau, Q. J., and Moore, J. P. (1993) *Philos. Trans. R. Soc. London (Biol.) 342*, 59−66.
3. Feng, Y., Broder, C. C., Kennedy, P. E., and Berger, E. A. (1996) *Science 272*, 872−877.
4. Deng, H. K., Liu, R., Ellmeier, W., Choe, S., Unutmaz, D., Burkhart, M., Di Marzio, P., Marmon, S., Sutton, R. E., Hill, C. M., Davis, C. B., Peiper, S. C., Schall, T. J., Littman, D. R., and Landau, N. R. (1996) *Nature 381*, 661−666.
5. Dragic, T., Litwin, V., Allaway, G. P., Martin, S. R., Huang, Y. X., Nagashima, K. A., Cayanan, C., Maddon, P. J., Koup, R. A., Moore, J. P., and Paxton, W. A. (1996) *Nature 381*, 667−673.
6. Alkhatib, G., Combadiere, C., Broder, C. C., Feng, Y., Kennedy, P. E., Murphy, P. M., and Berger, E. A. (1996) *Science 272*, 1955−1958.
7. Maddon, P. J., Littman, D. R., Godfrey, M., and Maddon, D. E. (1985) *Cell 42*, 93−104.
8. Moore, J. P., McKeating, J. A., Weiss, R. A., and Sattentau, Q. J. (1990) *Science 250*, 1139−1142.
9. Arthos, J., Deen, K. C., Chaikin, M. A., Fornwald, J. A., Sathe, H., Sattentau, Q. J., Clapham, P. R., Weiss, R. A., McDougal, J. S., Pietropaolo, C., Axel, R., Truneh, A., Maddon, P. J., and Sweet, R. W. (1989) *Cell 57*, 469−481.
10. Wang, J., Yan, Y., Garrett, T. P. J., Liu, J., Rodgers, D. W., Garlick, R. L., Tarr, G. E., Husain, Y., Reinherz, E. L., and Harrison, S. C. (1990) *Nature 348*, 411−418.
11. Ryu, S. E., Kwong, P. D., Truneh, A., Porter, T. G., Arthos, J., Rosenberg, M., Dai, X., Xuong, N. H., Axel, R., Sweet, R. W., and Hendrickson, W. A. (1990) *Nature 348*, 419−426.
12. Ryu, S.-E., Truneh, A., Sweet, R. W., and Hendrickson, W. A. (1994) *Structure 2*, 59−73.
13. Bachelder, R. E., Bilancieri, J., Lin, W., and Letvin, N. L. (1995) *J. Virol. 69*, 5734−5742.
14. Denisova, G., Raviv, D., Mondor, I., Sattentau, Q. J., and Gershoni, J. M. (1997) *J. Immunol. 158*, 1157−1164.
15. Moebius, U., Clayton, L. K., Abraham, S., Harrison, S. C., and Reinherz, E. L. (1992) *J. Exp. Med. 176*, 507−517.
16. Schockmel, G. A., Somoza, C., Davis, S. J., Williams, A. F., and Healy, D. (1992) *J. Exp. Med. 175*, 301−304.
17. Lazarus, R. A., and McDowell, R. S. (1993) *Curr. Opin. Biotechnol. 4*, 438−445.
18. Lee, G., Chan, W., Hurle, M. R., DesJarlais, R. L., Watson, F., Sathe, G. M., and Wetzel, R. (1993) *Protein Eng. 6*, 745−754.
19. Scandella, C. J., Kilpatrick, J., Lidster, W., Parker, C., Moore, J. P., Moore, G. K., Mann, K. A., Brown, P., Coates, S., Chapman, B., Masiarz, F. R., Steimer, K. S., and Haigwood, N. L. (1993) *AIDS Res. Hum. Retroviruses 9*, 1233−1244.
20. Pincus, S. H., Messer, K. G., Schwartz, D. H., Lewis, G. K., Graham, B. S., Blattner, W. A., and Fisher, G. (1993) *J. Clin. Invest. 91*, 1987−1996.
21. Pincus, S. H., Messer, K. G., and Hu, S.-L. (1994) *J. Clin. Invest. 93*, 140−146.
22. Pincus, S. H., Messer, K. G., Nara, P. L., Blattner, W. A., Colclough, G., and Reitz, M. (1994) *J. Clin. Invest. 93*, 2505.
23. Andrade, M. A., Chacon, P., Merelo, J. J., and Moran, F. (1993) *Protein Eng. 6*, 383−390.
24. Merelo, J. J., Andrade, M. A., Prieto, A., and Moran, F. (1994) *Neurocomputing 6*, 443−454.
25. Marion, D., and Wüthrich, K. (1983) *Biochem. Biophys. Res. Commun. 113*, 967−974.
26. Clore, G. M., and Gronenborn, A. M. (1983) *J. Magn. Reson. 53*, 423−442.
27. Campbell, A. P., and Sykes, B. D. (1993) *Annu. Rev. Biophys. Biomol. Struct. 22*, 99−122.
28. Ni, F., and Scheraga, H. A. (1994) *Acc. Chem. Res. 27*, 257−264.
29. Glaudemans, C. P. J., Lerner, L., Daves, G. D., Kovac, P., Venath, R., and Bax, A. (1990) *Biochemistry 29*, 10906−10911.
30. Davis, D. G., Perlman, M. E., and London, R. E. (1994) *J. Magn. Reson., Ser. B 104*, 266−275.
31. Bax, A., and Davis, D. G. (1985) *J. Magn. Reson. 65*, 355−360.
32. Zolnai, Z., Juranic, N., Markley, J. L., and Macura, S. (1995) *Chem. Phys. 200*, 161−179.
33. Nilges, M., Clore, G. M., and Gronenborn, A. M. (1988) *FEBS Lett. 239*, 129−146.
34. Jameson, B. A., Rao, P. E., Kong, L. I., Hahn, B. H., Shaw, G. M., Hood, L. E., and Kent, S. B. H. (1988) *Science 240*, 1335−1339.
35. London, R. E., Perlman, M. E., and Davis, D. G. (1992) *J. Magn. Reson. 97*, 79−98.
36. Landy, S. B., and Rao, B. D. N. (1989) *J. Magn. Reson. 81*, 371−377.
37. Macura, S., Westler, W. M., and Markley, J. L. (1994) *Methods Enzymol. 239*, 106−144.
38. Borgias, B. A., Gochin, M., Kerwood, D., and James, T. L. (1990) *Prog. Nucl. Magn. Reson. Spectrosc. 22*, 83−89.
39. Borgias, B. A., and James, T. L. (1990) *J. Magn. Reson. 87*, 475−487.
40. Wüthrich, K. (1986) *NMR of Proteins and Nucleic Acids*, pp 123−125, Wiley, New York.
41. Wagner, G., Neuhaus, D., Woergoetter, E., Vasak, M., Kaegi, J. H. R., and Wüthrich, K. (1986) *J. Mol. Biol. 187*, 131−135.
42. Dyson, H., Rance, M., Houghten, R., Lerner, R., and Wright, P. (1988) *J. Mol. Biol. 201*, 161−200.
43. Nara, P. L., Robey, W. G., Pyle, S. W., Hatch, W. C., Dunlop, N. M., Bess, J. W., Kelliher, J. C., Arthur, L. O., and Fischinger, P. J. (1988) *J. Virol. 62*, 2622−2628.
44. Javaherian, K., Langlois, A., McDanal, C., Ross, K. L., Eckler, L. I., Jellis, C. L., Profy, A. T., Rusche, J. R., Bolognesi, D. P., Putney, S. D., and Matthews, T. J. (1989) *Proc. Natl. Acad. Sci. U.S.A. 86*, 6768−6772.
45. Palker, T. J., Clark, M. E., Langlois, A. J., Matthews, T. J., Weinhold, K. J., Randall, R. R., Bolognesi, D. P., and Haynes, B. F. (1988) *Proc. Natl. Acad. Sci. U.S.A. 85*, 1932−1936.
46. Nara, P. L., Robey, W. G., Arthur, L. O., Asher, D. M., Wolff, A. V., Gibbs, C. J., Gajdusek, D. C., and Fischinger, P. J. (1987) *J. Virol. 61*, 3173−3180.
47. Daar, E. S., Li, X. L., Moudgil, T., and Ho, D. D. (1990) *Proc. Natl. Acad. Sci. U.S.A. 87*, 6574−6578.
48. Finberg, R. W., Wahl, S. M., Allen, J. B., Soman, G., Strom, T. B., Murphy, J. R., and Nichols, J. C. (1991) *Science 252*, 1703−1705.
49. Langejijk, J. P. M., Puijk, W. C., Vanhoorn, W. P., and Meloen, R. H. (1993) *J. Biol. Chem. 268*, 16875−16878.
50. Letvin, N. L., Chalifoux, L. V., Reimann, K. A., Ritz, J., Schlossman, S. F., and Lambert, J. M. (1986) *J. Clin. Invest. 78*, 666−673.
51. Haigwood, N. L., Barker, C. B., Higgins, K. W., Skiles, P. V., Moore, G. K., Mann, K. A., Lee, D. R., Eichberg, J. W., and Steimer, K. S. (1990) *Vaccines 90*, 313−320.
52. Haigwood, N. L., Nara, P. L., Brooks, E., VanNest, G. A., Ott, G., Higgins, K. W., Dunlop, N., Scandella, C. J., Eichberg, J. W., and Steimer, K. S. (1992) *J. Virol. 66*, 172−182.
53. Steimer, K. S., Scandella, C. J., Skiles, P. V., and Haigwood, N. L. (1991) *Science 254*, 105−108.
54. Brand, D., Srinivasan, K., and Sodroski, J. (1995) *J. Virol. 69*, 166−171.
55. Moore, J. P., Sattentau, Q. J., Wyatt, R., and Sodroski, J. (1994) *J. Virol. 68*, 469−484.
56. Wyatt, R., Sullivan, N., Thali, M., Repke, H., Ho, D., Robinson, J., Posner, M., and Sodroski, J. (1993) *J. Virol. 67*, 4557−4565.
57. Moore, J. P., and Sodroski, J. (1996) *J. Virol. 70*, 1863−1872.

58. O'Brien, W. A., Mao, S.-H., Cao, Y., and Moore, J. P. (1994) *J. Virol. 68*, 5264−5269.
59. Weber, P. C., Pantoliano, M. W., and Thompson, L. D. (1992) *Biochemistry 31*, 9350−9354.
60. Giebel, L. B., Cass, R. T., Milligan, D. L., Young, D. C., Arze, R., and Johnson, C. R. (1995) *Biochemistry 34*, 15430−15435.
61. Chen, S., Chrusciel, R. A., Nakanishi, H., Raktabutr, A., Johnson, M. E., Sato, A., Weiner, D., Hoxie, J., Saragovi, H. U., Greene, M. I., and Kahn, M. (1992) *Proc. Natl. Acad. Sci. U.S.A. 89*, 5872−5876.
62. Kwong, P. D., et al. (1998) *Nature 393*, 648−659.

BI980652O